J Nanostruct 16(2): 1862-1874, Spring 2026

RESEARCH PAPER

Halide-Dependent Optoelectronic Properties of $CsPbX_3$ Nanocomposite-Based Perovskite Solar Cells

Murtadha J. Edam [1], Shymaa K. Hussian [2], Rawaa Abbas Abd Ali [1], Samir M. AbdulAlmohsin [1]*

[1] *Department of Physics, College of Education for Pure Sciences, Thi-Qar University, Thi-Qar,64001, Iraq*

[2] *Department of Physics, College of Science, Al-Muthanna University, Al-Muthanna, Al-Samawa, 66001, Iraq*

ARTICLE INFO

Article History:
Received 20 October 2025
Accepted 18 March 2026
Published 01 April 2026

Keywords:
$CsPbX_3$
C60
Perovskite Solar Cells
SCAPS-1D
Simulation
SWCNT

ABSTRACT

In this work, we present results of all-inorganic Cs-based halide perovskite solar cells on three compositions: $CsPbI_3$, $CsPbBr_3$ and $CsPbCl_3$. The optical and photovoltaic performance was investigated by means of numerical simulations for different halide species. The device has a C_{60} ETL and an SWCNT HTL structure. The performance of $CsPbX_3$ (X = Cl or I) perovskites was found to strongly depend on the halide composition; among them, $CsPbI_3$ based device showed a record best efficiency (PCE = 19.9%, Jsc = 24.9 mA/cm², FF = 72%), suggesting its potential for high-efficiency applications.

How to cite this article
Edam M., Hussian S., Abd Ali R., AbdulAlmohsin S. Halide-Dependent Optoelectronic Properties of $CsPbX_3$ Nanocomposite-Based Perovskite Solar Cells. J Nanostruct, 2026; 16(2):1862-1874. DOI: 10.22052/JNS.2026.02.036

INTRODUCTION

There has been great interest in photovoltaic technologies, especially perovskite solar cells (PSCs), as promising candidates for next-generation solar cells compared to conventional silicon-based solar cells due to their high efficiency, low cost, and tunable bandgap [1-3]. Among them, all-inorganic cesium perovskite solar cells ($CsPbX_3$, X = I, Br, Cl) have been widely investigated owing to their high thermal stability and excellent long-term operational stability [4,5]. The optoelectronic properties of $CsPbX_3$ can be tuned by varying the halide composition, which strongly influences device performance [6-8].

Here, we develop a new device architecture using fullerene (C_{60}) as the electron transport layer (ETL) and single-walled carbon nanotubes (SWCNTs) as the hole transport layer (HTL), along with three different $CsPbX_3$ absorber compositions. The design aims at improving carrier transport, reducing recombination losses, and enhancing the power conversion efficiency (PCE). The photovoltaic characteristics of the designed cells were evaluated using SCAPS-1D simulations, including short-circuit current density (Jsc), open-circuit voltage (Voc), fill factor (FF), and power conversion efficiency (PCE).

* *Corresponding Author Email: shymaahussen@mu.edu.iq*

MATERIALS AND METHODS

The inorganic perovskite solar cell was simulated using SCAPS-1D, following the structure:

C_{60} / $CsPbX_3$ / SWCNT / Au.

C_{60} (ETL): Ensures efficient electron extraction and hole blocking.

$CsPbX_3$ (Absorber, X = I, Br, Cl): Main light-absorbing layer with tunable bandgap.

SWCNT (HTL): Provides stable, conductive pathways for hole transport.

Au (Back Contact): Offers high work function and stable hole collection.

Simulations were conducted under AM1.5G (1000 W/m²) illumination at 300 K, evaluating Jsc, Voc, FF, and efficiency (η).

Figs. 1A and B show the device structure and corresponding energy band alignment.

The simulated solar cell is composed of four functional layers as follows: C_{60} used as the electron transport layer (ETL); $CsPbX_3$, inorganic halide perovskite type, for the intrinsic layer absorbing the sunlight; SWCNT for hole transporting layer (HTL) and an Au back electrode. Two critical parameters, thickness and doping concentration determine each layer. A proper incorporation of the C SWCNT layer in the M3 structure ensures that excellent electron extraction and hole transport toward the rear contact are achieved. Photoactive "absorber" refers to a $CsPbX_3$ perovskite layer that is intrinsic (i.e. undoped). The back contact coverage with gold (Au) guarantees excellent charge collection and a good electrical back contact. The specific parameters of each layer are shown in Table 1.

RESULTS AND DISCUSSION

The C_{60} layer, as the ETL, has a moderate bandgap (2 eV) and high donor concentration (N_D = 10^{17} cm^{-3}), which is beneficial for efficient electron extraction and transport. The SWCNT (which works as the hole transport layer (HTL)) has a small bandgap of 0.9 eV and a large acceptor doping level (N_A = 10^{12}–10^{16} cm^{-3}), resulting in increased hole conduction [9,10].

Depending on the halide composition (I, Br direction: L, I) the absorber layer in $CsPbX_3$ absorbers shows greater variation in bandgap size and therefore gives way for a wider range of spectral tunability. The lack of doping numbers for

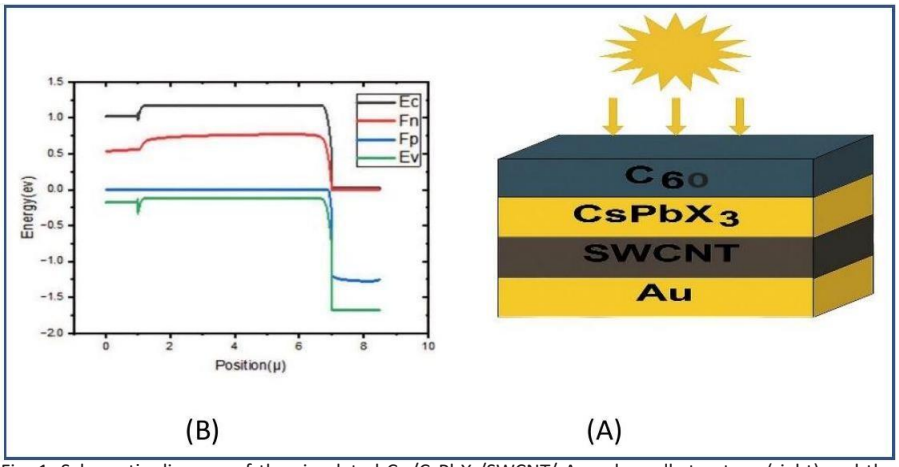

Fig. 1. Schematic diagram of the simulated C_{60}/$CsPbX_3$/SWCNT/ Au solar cell structure (right) and the corresponding energy band alignment (left) under standard AM1.5G illumination conditions.

Table 1. Thickness and doping parameters used in the C_{60}/$CsPbX_3$/SWCNT/ Au solar cell simulation.

Layer	Thickness (nm)	Band gap (ev) Eg	Acceptor density, N_A(1/cm^3)	Donor density, N_D (1/cm^3)
C_{60}	50	2	——	10^{17}
$CsPbI_3$	250	1.73	——	—–
$CsPbCL_3$	250	2.8	——	—-
$CsPbBr_3$	250	2.2	——	—–
SWCNT	400	0.9	10^{12} 10^{16}	—–

the absorber layers indicates that they are either intrinsic or slightly p-doped in order to minimize the recombination losses [11].

The simulation results indicate that the performance of the perovskite solar cell is strongly influenced by the thickness of the C_{60} electron transport layer. The highest power conversion efficiency (12.41%) is achieved at 10 nm, but ultra-thin layers may suffer from poor coverage and instability. Increasing the thickness beyond 50 nm leads to a decline in Voc, Jsc, FF, and efficiency due to higher series resistance and reduced charge extraction. At 200 nm, efficiency drops to 7.44%. Therefore, a thickness range of 20-50 nm

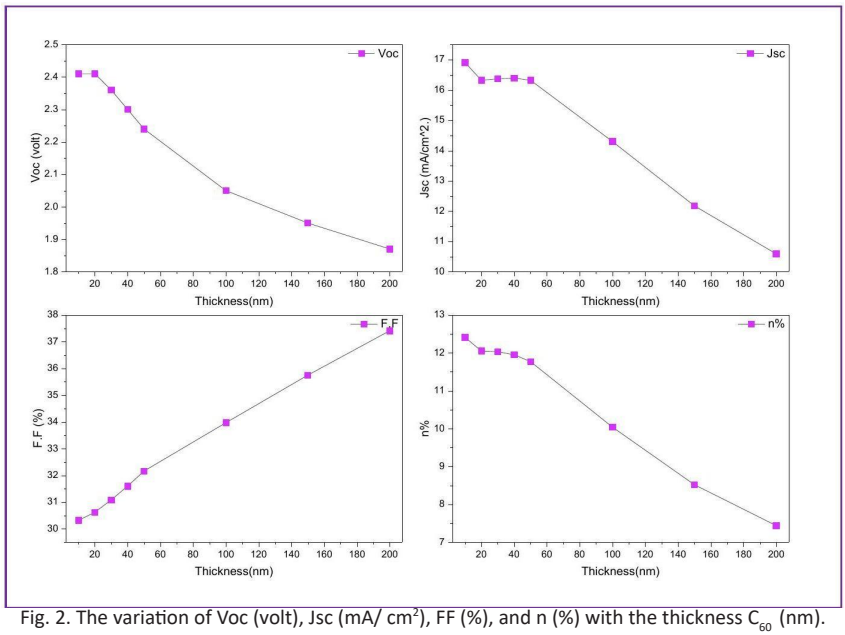

Fig. 2. The variation of Voc (volt), Jsc (mA/ cm^2), FF (%), and n (%) with the thickness C_{60} (nm).

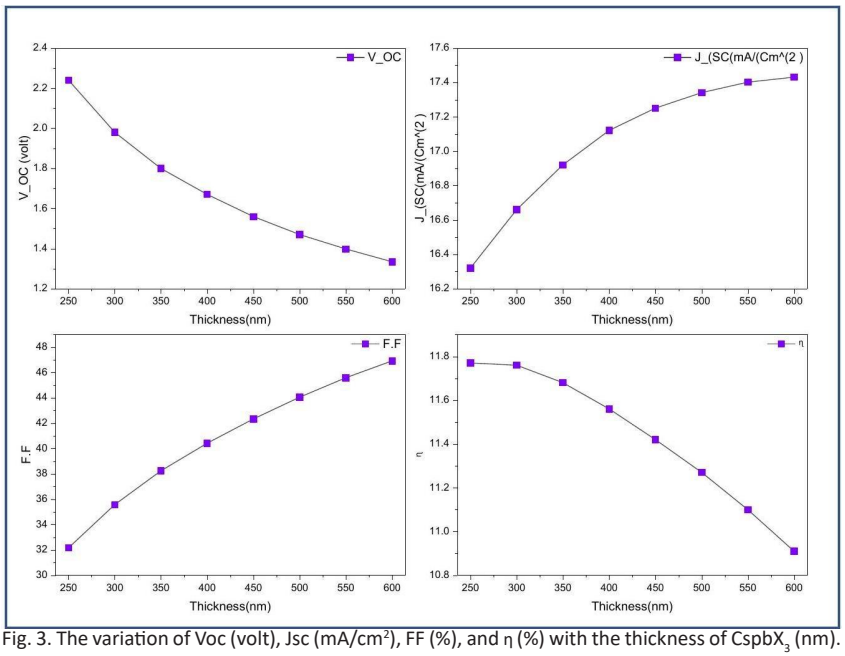

Fig. 3. The variation of Voc (volt), Jsc (mA/cm^2), FF (%), and η (%) with the thickness of $CspbX_3$ (nm).

is recommended to maintain a balance between efficiency and device stability [12].

The performance of the solar cell is affected by the thickness of the $CsPbX_3$ perovskite layer. As thickness increases from 250 to 600 nm, both Jsc and FF improve due to better light absorption, while Voc gradually decreases because of enhanced recombination in thicker layers. The highest efficiency (11.77%) is recorded at 250 nm, then it declines beyond 450 nm despite the rise

Table 2. Effect of C_{60} Layer Thickness on Solar cell performance parameters.

Thickness (nm) C_{60}	V_{OC} (VOLT)	Jsc(mA/cm^2)	FF (%)	N (%)
10	2.41	16.91	30.32	12.41
20	2.41	16.32	30.62	12.05
30	2.36	16.37	31.08	12.03
40	2.30	16.39	31.60	11.95
50	2.24	16.32	32.16	11.77
100	2.05	14.30	33.97	10.04
150	1.95	12.18	35.75	8.52
200	1.87	10.59	37.41	7.44

Table 3. Effect of $Cspbx_3$ Layer Thickness on Solar Cell Performance Parameter.

Thickness(nm) $Cspbx_3$	V_{OC} (volt)	J_{SC} (mA/Cm^2)	F.F (%)	η (%)
250	2.24	16.32	32.16	11.77
300	1.98	16.66	35.57	11.76
350	1.80	16.92	38.24	11.68
400	1.67	17.12	40.42	11.56
450	1.56	17.25	42.34	11.42
500	1.47	17.34	44.06	11.27
550	1.398	17.401	45.59	11.10
600	1.334	17.43	46.92	10.91

$Jsc\ \left(\frac{mA}{Cm^2}\right)$

Table 4. Effect of SWCTN Layer Thickness on Solar Cell Performance Parameters.

Thickness (nm) SWCNT	V_{OC} (volt)	J_{SC} (mA/Cm^2)	FF (%)	η (%)
50	2.46	16.24	30.08	12.03
100	2.43	16.57	30.29	12.21
150	2.43	16.75	30.23	12.32
200	2.43	16.83	30.18	12.37
250	2.43	16.87	30.16	12.39
300	2.43	16.88	30.13	12.40
350	2.43	16.89	30.13	12.40
400	2.43	16.89	30.13	12.40

in Jsc and FF, indicating a tradeoff caused by Voc reduction.

Therefore, a thickness range of 250−400 nm is recommended to achieve balanced efficiency, light absorption, and device stability [13].

The simulation results demonstrate that the power conversion efficiency (PCE) of the solar cell improves with increasing the thickness of the SWCNT layer, reaching a maximum value of 12.40% at thicknesses of 300 nm,350 nm, and 400 nm. This enhancement in efficiency is attributed to the improved charge transport and hole collection capability provided by the thicker SWCNT layer, which reduces series resistance and enhances the short-circuit current density (J_{SC}) without compromising the open-circuit voltage (V_{OC}). Beyond a certain threshold, the efficiency appears to saturate, indicating that further thickness increase beyond 300 nm does not yield additional performance gains. Therefore, a thickness in the range of 300−400 nm is considered optimal for maximizing device performance [14].

Analysis of the Solar Cell Structure Using C_{60}, SWCNT, and Perovskite Layers

In this solar cell configuration, the structure was designed to include fullerene (C_{60}) as the electron transport layer (ETL), single-walled carbon nanotubes (SWCNT) as the hole transport layer (HTM), and a perovskite absorber layer. The

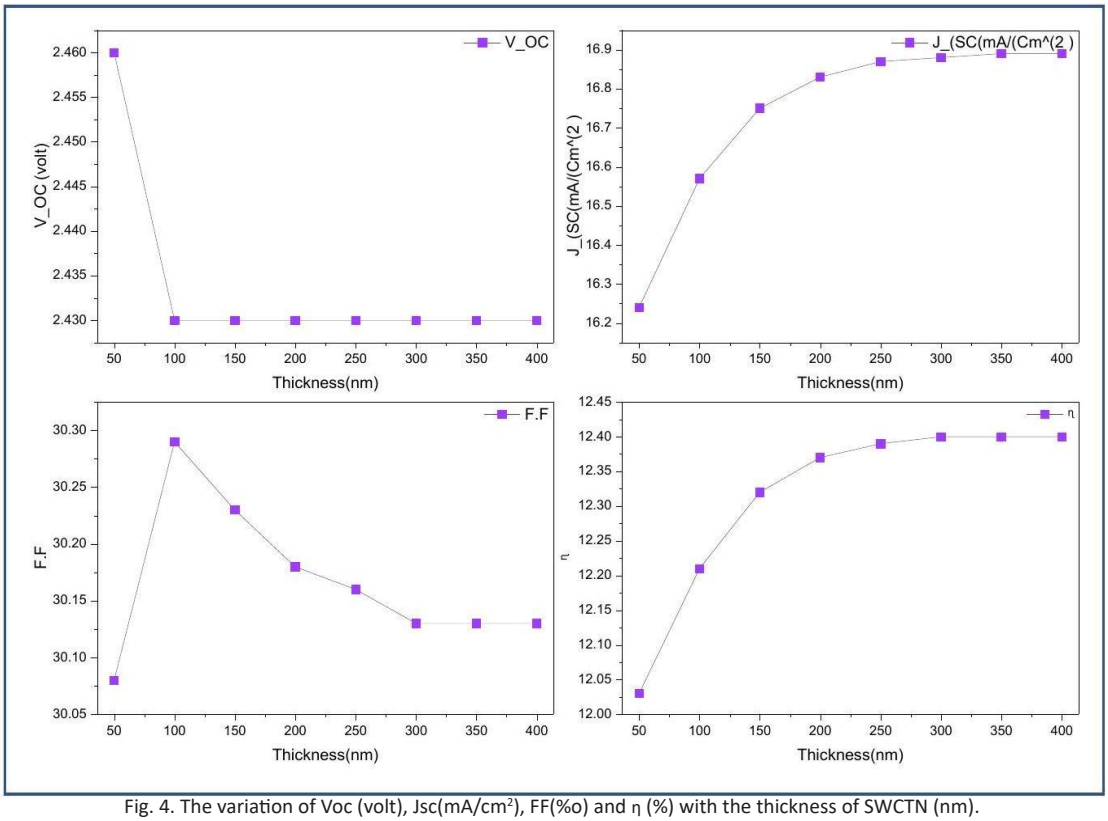

Fig. 4. The variation of Voc (volt), Jsc(mA/cm^2), FF(%o) and η (%) with the thickness of SWCTN (nm).

Table 5. Selected Optimal Thicknesses.

Layer	Optimal Thickness (nm)	Achieved Efficiency (%)
C_{60}	50	11.77
SWCNT	300-350-400	12.40
Perovskite	250	11.77

optimal thickness for each layer was selected based on the highest achieved power conversion efficiency. (PCE), as determined through SCAPS-1D simulations.

The selected parameters and their corresponding efficiencies are summarized in the Table 5.

These thickness values were applied in a simulated solar cell structure in SCAPS, while other parameters were kept constant.

Effect of Temperature on Solar Cell Performance

The performance of the solar cell was analyzed using SCAPS-1D over a temperature range of 283− 343 K. The structure included a C_{60} electron transport layer, a perovskite absorber, and an

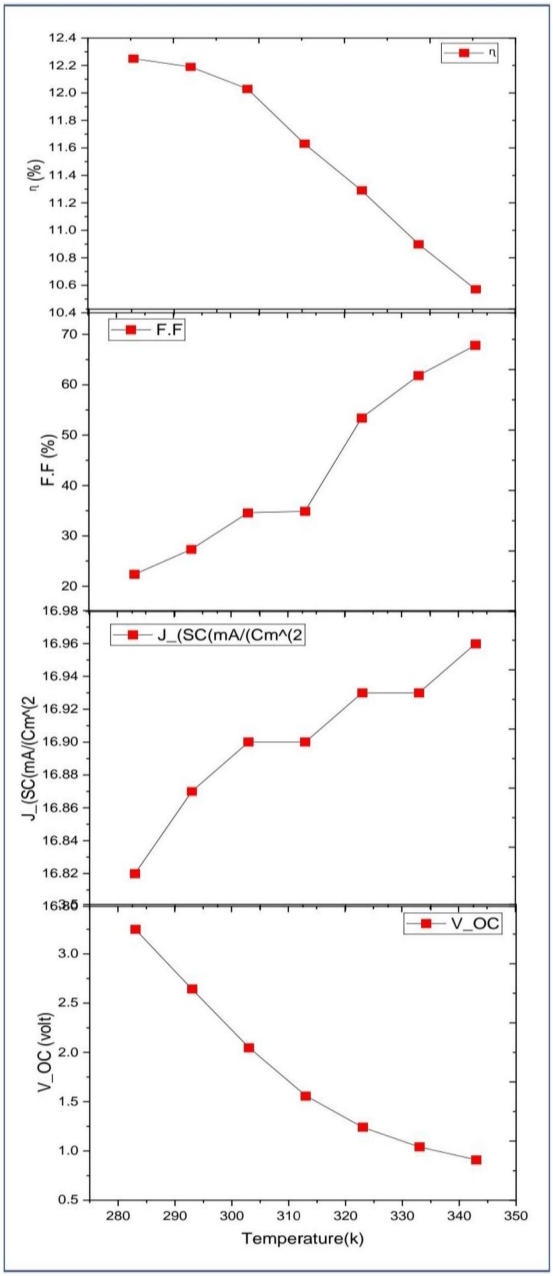

Fig. 5. Effect of Temperature on Voc, Jsc, Fill Factor, and Efficiency of the Solar Cell.

SWCNT hole transport layer. The open-circuit voltage (Voc) dropped significantly from 3.25 V to 0.91 V with rising temperature due to increased recombination. In contrast, the short-circuit current density (Jsc) remained nearly constant, indicating minimal impact on light absorption and charge generation. The fill factor (FF) improved notably from 22.35% to 67.85%, suggesting better charge extraction and reduced internal losses. Despite the Voc drop, the enhanced FF helped maintain a relatively high-power conversion efficiency (η), which only slightly decreased from 12.25% to 10.57%.

This table demonstrates the impact of temperature on solar cell efficiency, which is consistent with previous findings reported in the literature [4].

The results show that increasing temperature negatively affects the solar cell performance by significantly reducing the open-circuit voltage (V_{OC}) and efficiency (η), due to the rise in reverse saturation current. Meanwhile, the short-circuit current density (Jsc) and fill factor (FF) slightly increase as a result of improved charge mobility and reduced internal resistance. However, the drop in voltage dominates, leading to an overall decline in efficiency.

The Role of Band Gap in $CsPbX_3$ Layer Performance

The band gap plays a key role in determining the efficiency of the $CsPbX_3$ perovskite layer by affecting its ability to absorb light and generate charge carriers. Proper control of the band gap enhances solar spectrum absorption and improves compatibility with other cell components, leading to better performance and stability. Approximate band gap values based on halogen type

$CsPbCl_3$ ≈ 3.0eV, $CsPbBr_3$ ≈ 2.3eV, and $CsPbI_3$ ≈ 1.73eV.

The results showed that increasing the energy band gap in $CsPbI_3$ solar cells leads to a gradual rise in the open-circuit voltage (Voc) but a decrease in the short-circuit current density (Jsc). Nevertheless, the fill factor (FF) and efficiency (η)

Table 6. Simulation Results.

Layer Configuration	V_{OC} (Volt)	J_{SC} (mA/Cm^2)	FF (%)	n (%)
C_{60} (50 nm) + SWCNT (350 nm) + Perov. (250nm)	2.223	16.89	32.18	12.09

Table 7. Temperature Dependence of Solar Cell Performance.

Temperature (k)	V_{OC} (volt)	J_{SC} (mA/Cm^2)	FF (%)	η (%)
283	3.25	16.82	22.35	12.25
293	2.64	16.87	27.33	12.19
303	2.05	16.90	34.60	12.03
313	1.56	16.90	34.88	11.63
323	1.24	16.93	53.45	11.29
333	1.04	16.93	61.85	10.90
343	0.91	16.96	67.85	10.57

Table 8. Effect of Energy Band Gap on the Performance of

Energy band gap (ev) $CsPbCl_3$	V_{OC} (Volt)	J_{SC} (mA/Cm^2)	FF (%)	n (%)
2.8	2.0	10.5	68.0	5.5
2.9	2.05	9.8	66.5	5.0
3.0	2.1	9.0	65.0	4.5
3.1	2.15	8.2	63.0	4.0
3.2	2.2	7.5	60.0	3.5

remained relatively stable. It can be concluded that an energy band gap between 1.7 and 1.75 eV offers an optimal balance for cell performance [15-17].

The results indicate that the energy band gap of the SWCNT layer has a minimal effect on the photovoltaic performance of the solar cell. As the band gap increases from 0.8 eV to 1.5 eV , the short-circuit current density (Jsc) remains constant at 15.81 mA/cm^2, and both the fill factor (FF) and

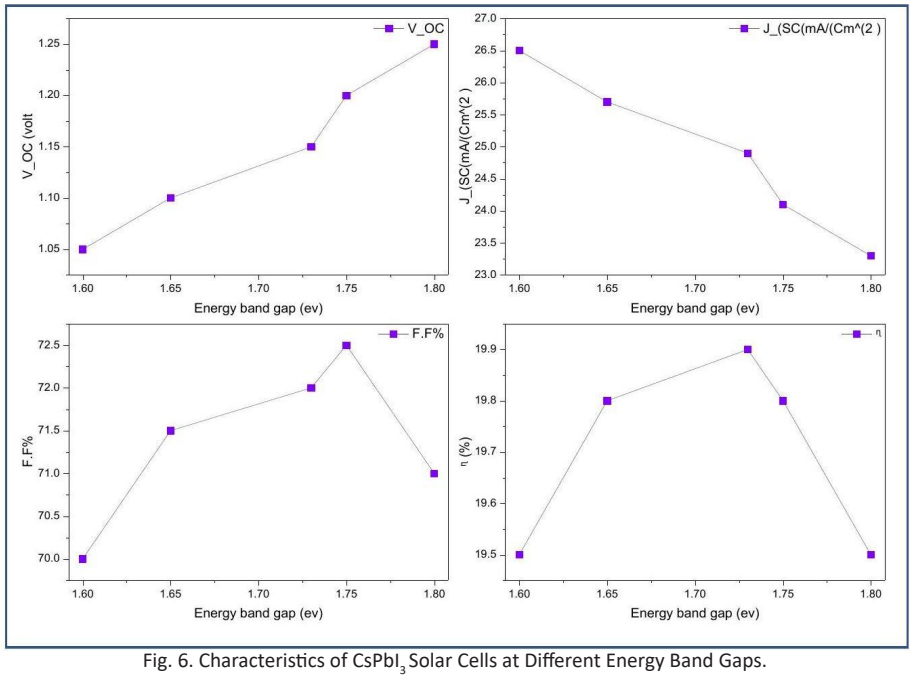

Fig. 6. Characteristics of $CsPbI_3$ Solar Cells at Different Energy Band Gaps.

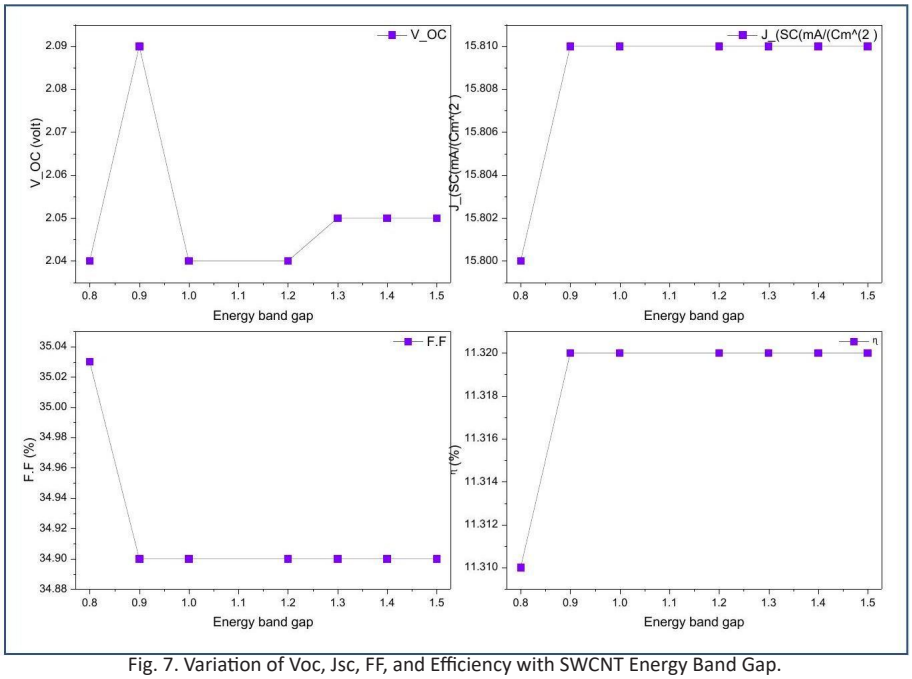

Fig. 7. Variation of Voc, Jsc, FF, and Efficiency with SWCNT Energy Band Gap.

the efficiency (η) stay nearly unchanged at 34.9% and 11.32%, respectively. A slight increase in the open-circuit voltage (Voc)is observed at 0.9 eV , but it does not significantly influence the overall performance.

This stability may be attributed to the fact that the SWCNT layer acts as an efficient hole transport material within this range of band gaps, minimizing the influence of slight energy band gap variations on device performance. Additionally, charge transport in this layer is not highly dependent on the band gap width within this narrow range, which leads to relatively stable solar cell behavior [18].

Table 9. Effect of Energy Band Gap on the Performance of $CsPbBr_3$ Solar Cells.

Energy band gap (ev) $CsPbBr_3$	V_{OC} (volt)	J_{SC} (mA/Cm^2)	FF (%)	n (%)
2.2	1.6	17.5	70.0	13.0
2.25	1.65	16.8	69.5	12.8
2.3	1.7	16.0	68.0	12.5
2.35	1.75	15.3	66.0	12.0
2.4	1.8	14.5	64.0	11.5

Table 10. Effect of Energy Band Gap on the Performance of $CsPbI_3$ Solar Cells.

Energy band gap (ev) $CsPbI_3$	V_{OC} (volt)	J_{SC} (mA/Cm^2)	FF (%)	n (%)
1.6	1.05	26.5	70.0	19.5
1.65	1.1	25.7	71.5	19.8
1.73	1.15	24.9	72.0	19.9
1.75	1.2	24.1	72.5	19.8
1.8	1.25	23.3	71.0	19.5

Table 11. Influence of SWCNT Energy Band Gap on Photovoltaic Performance Parameters (Voc, Jsc, FF, η).

Energy band gap (ev) $CsPbI_3$	V_{OC} (volt)	J_{SC} (mA/Cm^2)	FF (%)	n (%)
1.6	1.05	26.5	70.0	19.5
1.65	1.1	25.7	71.5	19.8
1.73	1.15	24.9	72.0	19.9
1.75	1.2	24.1	72.5	19.8
1.8	1.25	23.3	71.0	19.5

Table 12. Effect of C_{60} Energy Band Gap on Photovoltaic Parameters (voc, Jsc, FF, η) of Solar Cell.

Energy band gap C_{60}	V_{OC} (Volt)	J_{SC} (mA/Cm^2)	FF (%)	n (%)
1.5	0.92	16.5	62.1	9.50
1.6	1.58	16.63	41.15	10.86
1.7	2.01	16.76	34.48	11.61
1.8	2.22	16.89	32.1	12.09
1.9	2.37	16.9	30.58	12.36
2	2.50	17.0	29.32	12.56

As the energy band gap of the C_{60} layer increases from 1.5 eV to 2 eV , the overall power conversion efficiency (η) of the solar cell improves steadily from 9.50% to 12.56%. This enhancement is mainly attributed to the increase in open-circuit voltage (Voc) and short-circuit current density (Jsc)

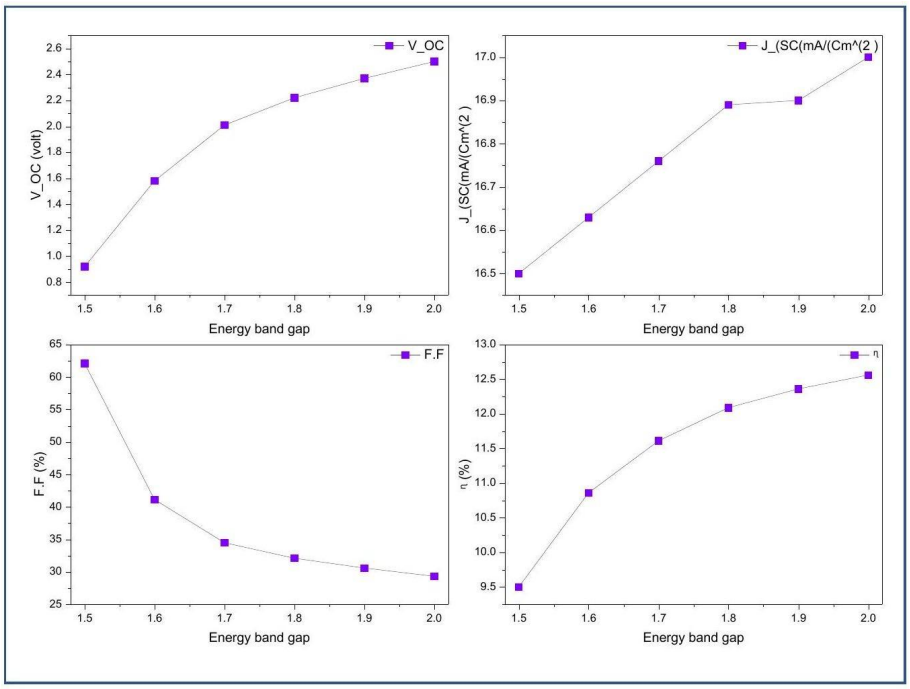

Fig. 8. Effect of energy gap on Voc, Jsc, FF and efficiency.

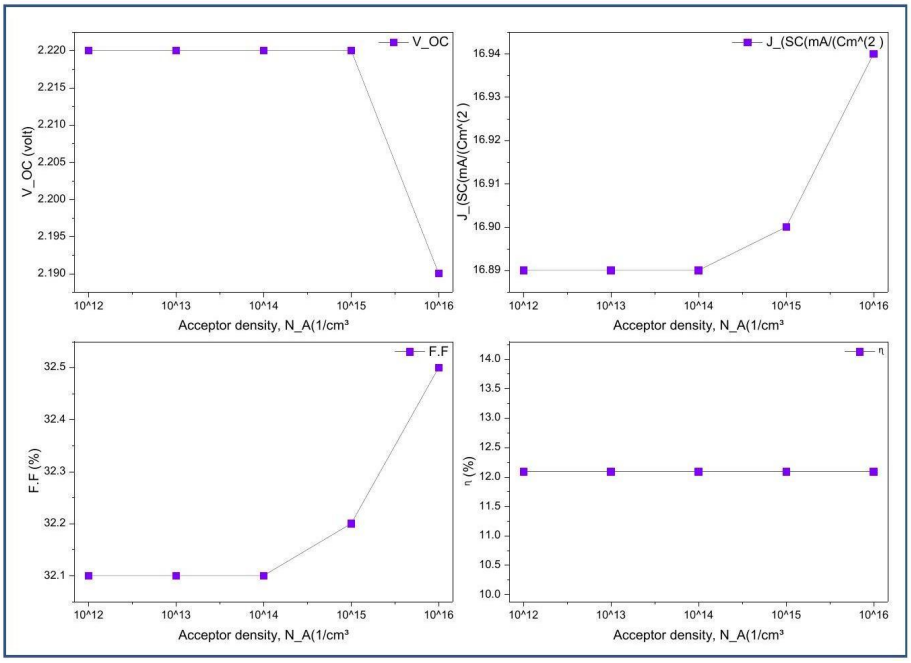

Fig. 9. Variation of SWCNTs layer Parameters with Increasing Acceptor Density (N_A).

with higher band gaps. Although the fill factor (FF) slightly decreases, its impact is offset by the larger gains in Voc and Jsc, indicating that optimizing the band gap of the electron transport layer (ETL) is crucial for improving device performance [19].

The results showed that the power conversion efficiency (η) remained nearly constant at approximately 12.09% despite the increase in acceptor density (N_A) in the SWCNT layer from 10^{12} to 10^{16} cm^{-3}. This stability can be attributed to the fact that the doping level was sufficient to enhance the electrical conductivity of the SWCNTs without

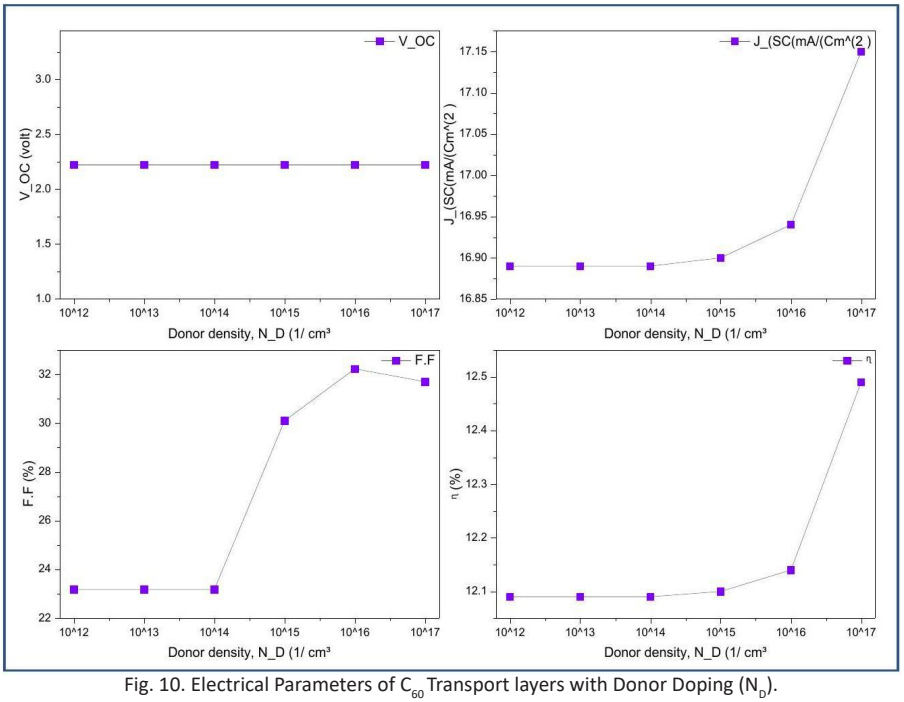

Fig. 10. Electrical Parameters of C_{60} Transport layers with Donor Doping (N_D).

Table 13. Effect of Acceptor Density (N_A) on the Performance of SWCNTs layer.

Acceptor density, N_A(1/cm^3)	V_{OC} (volt)	J_{SC} (mA/Cm^2)	FF (%)	η (%)
10^{12}	2.22	16.89	32.1	12.09
10^{13}	2.22	16.89	32.1	12.09
10^{14}	2.22	16.89	32.1	12.09
10^{15}	2.22	16.90	32.2	12.09
10^{16}	2.19	16.94	32.5	12.09

Table 14. Electrical Parameters of C_{60} Transport layers with Donor Doping (N_D).

Donor density, N_D(1/cm^3)	V_{OC} (volt)	J_{SC} (mA/Cm^2)	FF (%)	η (%)
10^{12}	2.22	16.89	23.18	12.09
10^{13}	2.22	16.89	23.18	12.09
10^{14}	2.22	16.89	23.18	12.09
10^{15}	2.22	16.90	30.1	12.1
10^{16}	2.22	16.94	32.23	12.14
10^{17}	2.22	17.15	31.7	12.49

turning them into a fully conductive (metallic) material. Such moderate doping improved hole transport and led to slight enhancements in the fill factor (FF) and short-circuit current density (Jsc), but these improvements were not significant enough to noticeably affect the overall efficiency. Therefore, it can be concluded that an optimal doping level exists, which enhances the performance of the layer while preserving the semiconducting properties essential for efficient solar cell operation. [8, 20, 21].

The results indicate that increasing the donor density (N_D) in the C_{60} transport layer from 10^{12} to 10^{17} cm^{-3} led to a noticeable improvement in solar cell performance. The short-circuit current density (Jsc) increased from 16.89 to 17.15 mA/cm^2, the fill factor (FF) improved from 23.18% to 31.7%, and the power conversion efficiency (η) rose from 12.09% to 12.49%, while the open-circuit voltage (Voc) remained constant at 2.22 V . This enhancement is attributed to better electrical conductivity of the C_{60} layer with higher N_D, which facilitated electron transport and reduced series resistance. However, the improvement remains moderate, suggesting that there is an optimal doping level that should not be exceeded to maintain the semiconducting properties of the layer.

CONCLUSION

The proposed inorganic perovskite solar cell structure incorporating C60 as the electron transport layer (ETL) and SWCNT as the hole transport material (HTL) achieved a power conversion efficiency (PCE) of 19.9%. The selected perovskite absorber exhibited a suitable energy bandgap, enabling efficient light absorption and effective carrier generation. Optimization of the layer thickness played a crucial role in maximizing device performance. Furthermore, reducing the defect density significantly suppressed recombination losses and improved charge transport. The use of a low work function back-contact metal enhanced charge extraction efficiency, while moderate doping levels in the transport layers improved charge separation and reduced recombination. Overall, the C_{60}/SWCNT configuration demonstrates strong potential for developing high-efficiency and stable inorganic perovskite solar cells.

CONFLICT OF INTEREST

The authors declare that there is no conflict of interests regarding the publication of this manuscript.

REFERENCES

1. Ranjan R, Anand N, Tripathi MN, Srivastava N, Sharma AK, Yoshimura M, et al. SCAPS study on the effect of various hole transport layer on highly efficient 31.86% eco-friendly CZTS based solar cell. Sci Rep. 2023;13(1).
2. Park H-J, Son H, Jeong B-S. SCAPS-1D Simulation for Device Optimization to Improve Efficiency in Lead-Free CsSnI3 Perovskite Solar Cells. Inorganics. 2024;12(4):123.
3. Mohd Alias NSN, Arith F, Mustafa AN, Ismail MM, Azmi NF, Saidon MS. Impact of Al on ZnO Electron Transport Layer in Perovskite Solar Cells. Journal of Engineering and Technological Sciences. 2022;54(4):220409.
4. Abbas Abd Ali R, K. Hussian S. Bandgap engineering and toxicity Mitigation in CsPb(BrxCly) mixed-halide perovskite thin films and nanoparticles via Sn2+ substitution. Solid State Commun. 2025;406:116185.
5. Wahid MF, Das U, Paul BK, Paul S, Howlader MN, Rahman MS. Numerical Simulation for Enhancing Performance of MoS_2 Hetero-Junction Solar Cell Employing Cu_2O as Hole Transport Layer. Materials Sciences and Applications. 2023;14(09):458-472.
6. Wang X, Yang X, Hu M, Liu H, Liu S, Zhou X. Corrosion behavior of pressureless-sintered SiC in molten NaCl–KCl–MgCl2 salt at 700 °C. Sol Energy Mater Sol Cells. 2022;242:111771.
7. Extended Dual-Functional Engineering for High-Performance 2D DionJacobson CsPbI3 Perovskite Solar Cells with Enhanced Stability. American Chemical Society (ACS).
8. Becker JJ, Campbell CM, Tsai C-Y, Zhao Y, Lassise M, Zhao X-H, et al. Monocrystalline 1.7-eV-Bandgap MgCdTe Solar Cell With 11.2% Efficiency. IEEE Journal of Photovoltaics. 2018;8(2):581-586.
9. Oublal E, Ait Abdelkadir A, Sahal M. High performance of a new solar cell based on carbon nanotubes with CBTS compound as BSF using SCAPS-1D software. J Nanopart Res. 2022;24(10).
10. Oublal E, Al-Hattab M, Ait Abdelkadir A, Sahal M. New numerical model for a 2T-tandem solar cell device with narrow band gap SWCNTs reaching efficiency around 35 %. Solar Energy. 2022;246:57-65.
11. Castrucci P. Carbon nanotube/silicon hybrid heterojunctions for photovoltaic devices. Advances in nano research. 2014;2(1):23-56.
12. AbdulAmohsin SM, Cui JB, Mohammed MZ. Study on ZnO/P3HT:PCBM nanowire solar cells. 2013 IEEE 39th Photovoltaic Specialists Conference (PVSC); 2013/06: IEEE; 2013. p. 2685-2689.
13. Otalora CA, Loaiza A, Gordillo G. Improvement of the properties of P3HT: PCBM blends using new solvents. 2013 IEEE 39th Photovoltaic Specialists Conference (PVSC); 2013/06: IEEE; 2013. p. 2746-2751.
14. AbdulAlmohsin S, Armstrong J, Cui JB. CdS nanocrystal-sensitized solar cells with polyaniline as counter electrode. Journal of Renewable and Sustainable Energy. 2012;4(4).
15. Zainab RA, Samir MA. High Efficiency Solar Cells Base on Organic-inorganic Perovskites Materials. University of Thi-Qar Journal of Science. 2021;8(2):23-29.
16. Preparation of Nanoporous MgO-Coated TiO_2 Nanoparticles and Their Application to the Electrode of Dye-Sensitized Solar Cells. American Chemical Society (ACS). http://dx.doi.org/10.1021/la051807d.s001

17. High Efficiency Solar Cells Base on Organic-inorganic Perovskites Materials. University of Thi-Qar Journal of Science. 2021:23-29.
18. Highest Efficiency of Perovskite Structure Solar Cells. International Journal of Thin Film Science and Technology. 2024;13(1):37-45.
19. Rshash HA, Almohsin SMA. Optimization of Temperature, Defects, and Thickness for High Efficiency of Tin Halide Perovskites. Journal of Education for Pure Science-University of Thi-Qar. 2024;14(2).
20. Hamadi GM, Lafta SF. Immunological parameters of recurrent miscarriages among women in Thi-Qar province. J Med Life. 2022;15(5):635-639.
21. Liu C, Yang Y, Zhang C, Wu S, Wei L, Guo F, et al. Tailoring C60 for Efficient Inorganic CsPbI2Br Perovskite Solar Cells and Modules. Adv Mater. 2020;32(8).